AIMS *Energy*

Research article

Design of a hybrid wind-solar street lighting system to power LED lights on highway poles

Nadwan Majeed Ali* and Handri Ammari

Department of Mechanical Engineering, Mutah University, Mutah, Karak 61710, Jordan

* **Correspondence:** Email: Nadwanmajeed2016@gmail.com; Tel: +9647711815335.

Abstract: This is an experimental study that investigates the performance of a hybrid wind-solar street lighting system and its cost of energy. The site local design conditions of solar irradiation and wind velocity were employed in the design of the system components. HOMER software was also used to determine the Levelized Cost of Energy (LCOE) and energy performance indices, which provides an assessment of the system's economic feasibility. The hybrid power supply system comprised of an integrated two photovoltaic (PV) solar modules and a combined Banki-Darrieus wind turbines. The second PV module was used to extend the battery storage for longer runtime, and the Banki-Darrieus wind turbines were used also to boost the battery charge for times when there is wind but no sunshine, especially in winter and at night. The results indicated that the hybrid system proved to be operating successfully to supply power for a street LED light of 30 watts. A wind power of 113 W was reached for a maximum wind speed that was recorded in the year 2021 of 12.10 m/s. The efficiency of the combined Banki-Darrieus wind turbine is 56.64%. In addition, based on the HOMER optimization analysis of three scenarios, of which, using either a solar PV system or the combined wind turbines each alone, or using the hybrid wind-solar system. The software results showed that the hybrid wind-solar system is the most economically feasible case.

Keywords: solar energy; wind energy; hybrid system; LED streetlight; HOMER

Abbreviations: DOD: Depth of Discharge; CFL: Compact Fluorescent Lamp; LED: Light Emitting

Diode; SCC: Short Circuit Current; PV: Photovoltaic; AD: Autonomy Days; A_ω: Rotor Wind Blades Swept Area (m^2); B_Loss: Battery Loss Factor; C_P: Wind Turbine Power Coefficient; P_Peak: Peak Power of PV Module; BAC: Battery Amperage Capacity; LCOE: Levelized Cost of Energy; O&M: Operation and Maintenance; PBP: Pay-Back Period; LF: Losses Factor; PR: Performance Ratio; CCC: The Charge Controller Current; DHL: Daily Hourly Load; DL: Daily Load; DOD: Depth of Discharge; NS: Number of Strings; NV: Nominal Voltage of the Battery; P: Wind Electrical Power (kW); PR: Performance Ratio; PVW: Solar PV Wattage; SCC: The Short Circuit Current; SDH: Sun Daily Hours; WTC: Wind Turbine Capacity; R: Radius of Banki Turbine

1. Introduction

Energy storage systems are used to help save an excess generation of clean electrical power from different renewable energy resources to be used later at periods when no adequate renewable energy resources are available. In the last three decades, hybrid energy systems were developed and innovated as a response to solar and wind energy resources utilization. For instance, hybrid energy systems can be used in places, where the electricity tariff of the electrical grid is highly expensive, and in locations, where the electrical grid is weak and intermittent, or at times when solar radiation is weak, as well as wind energy is not sufficient to generate clean electrical power.

Many papers have been published in recent years with increasing attention to hybrid systems of renewable energy.

Khare, V. et.al [1] used hybrid energy systems that are featured with their high capability to increase the rate of reliability of several renewable energy systems. They investigated experimentally the economic feasibility of a hybrid wind-solar energy system to offer clean electrical power for street lighting in low-traffic roads, in which, they sized the wind turbine, solar PV modules, batteries, charge controller, and converter. They selected metal halide lamps as they are the most appropriate light bulbs for low-traffic roads. Their results revealed that solar and wind energy resources can be utilized to operate low-consuming streetlights. In addition, findings confirmed that the annual energy generation equaled 371.7 kWh, whereas the annual energy consumption amounted to 222.8 kWh. Consequently, the remaining amount (148.9 kWh) could be exported to the electrical network making a profit from the hybrid wind-solar energy system.

Al-Tarawneh [2] focused on experimental research to calculate the annual cost savings and payback period of using LED streetlights powered via solar PV modules, Al-Tarawneh's experimental work revealed that using LED lights operated by PV power can achieve energy savings of 65% and annual energy savings of 484,261 JD, ($1 = 0.71 JD), for five major streets in Jordan. In addition, the payback period of the renewable energy system for streetlights equaled 1.47 years.

Mazzeo, H. et al., [3] examined the dynamic and energy reliability analysis of renewable hybrid system consisting of a photovoltaic solar generator, a wind micro generator and an electric generator with a storage battery to supply power for a heat pump. The heat pump is employed for heating and cooling air-conditioning of an office building environment. The dynamic simulation results identified the most contemporary load compared with the availability of the renewable source and determined the system energy reliability.

Elmorshedy, et al., [4] proposed in their study a joint and conceptual approach for techno-economic and dynamic rule-based power control of an off-grid solar—wind renewable energy system. Their design results indicated that the hybrid renewable energy system, which integrated solar, wind,

lead-acid batteries, and converter with optimal capacities of 55 kW, 18 kW, 325 kW and 42 kW, respectively, is the most cost-effective alternative with the minimum net present and energy costs of $232,423.3 and $0.3458/kWh, respectively.

Mazzeo, D. et al., [5] reviewed and made statistical analysis starting from data extracted from recent articles concerning hybrid systems. The goal of the review was to create an upgradable matrix literature database that categorizes the content of all articles into categories like geographical distribution, component configurations, operating mode and auxiliary components used to support it, intended uses, study methodologies (simulation, experimental, economic, energy, environmental, and social analysis, and so on) and software used. Furthermore, all optimization algorithms, energy, economic, environmental, and social indicators available in the literature were extracted and elaborated in order to identify the most commonly used.

Wadi, M. [6] investigated a case study of a hybrid wind-solar energy system to offer electrical power for street lighting in Turkey. He utilized a hybrid energy system and fuzzy control to control the operation and production of streetlights. The aim was to control the LED light intensity according to the battery voltage and wind speed.

Ricci, R. [7] used a hybrid renewable energy system, which integrated solar, wind, lead-acid batteries and inverter, and created optimal capacities of 55 kW, 18 kW, 325 kW and 42 kW, respectively. The most cost-effective alternative with the minimum net current energy costs were $232, $423.3 and $0.3458/kWh, respectively.

Georges, S. & Slaoui, F. [8] made a comparative study between LED and high-pressure sodium light bulbs. They made an analysis to size and design each component of a hybrid wind-solar energy system, which included wind turbines, solar PV panels, Gel batteries and charge controllers. The results indicated that using 40 kW solar PV system and 40 kW wind system for 80 Watt—1,000 LED street costs $80,000. Moreover, replacing high-pressure sodium bulbs with 80 Watt LED can achieve $2.66 savings in the initial installed cost of streetlights.

Al-Sarraj, et, al. [9] conducted a study aiming to assess the economic viability related to the use of a hybrid solar and wind energy system to provide clean electrical power for a facility in Iraq. They used HOMER software to estimate the hybrid system's economic feasibility. Their analysis results revealed that power produced from the solar PV system is 61.6 kW/annum, while the power from wind is 2.7 kW/annum.

This experimental study will highlight the beneficial effects and primary responsibilities of hybrid energy systems in achieving energy security, sustainability and reliability of wind PV solar systems for street lighting. The work will attempt to provide enough electric power to eliminate the need for electric power from the national electric grid, which can help save money and manpower for operation and maintenance (O&M) and reduce carbon emissions with reliable LED lighting. Moreover, HOMER software was used to analyze a similar system that uses solar and wind energy to provide electrical power for LED street lights. The LCOE, which is defined as an investment index that described the total price of energy provided by the renewable energy system by dividing the total initial cost by the annual savings, was calculated to determine the economic viability of the entire system.

2. Research methodology

The following main methodological steps were conducted in carrying out this study:

- A review, field survey, and analysis of energy demand for street lighting of past relevant applications were carried out.
- Analysis and assessment of the wind and solar radiation energy potential at the geographical location of the experimental setup were conducted.
- An estimation of the PV system size and design of the combined wind turbine system were made.
- The experiments and measurements were performed to check the success of the operation of the hybrid system in street lighting.
- The HOMER software was used in order to check the economic feasibility of the hybrid wind-solar system.

3. Design and performance analysis

To calculate the clean electrical power value produced from the wind turbine, the following equation is used [10]:

$$P = \frac{1}{2} \rho C_P A_\omega v^3 \tag{1}$$

where P is the wind electrical power, ρ is the air density, C_P is the wind turbine power coefficient, A_ω is the wind turbine blades swept area, and v is the wind speed. To calculate the wind turbine power required to feed the load of the streetlight, Eq 2 is used [11]:

$$WTC = \frac{\pi}{2} \times r^2 \times v^3 \times \rho \times \eta \tag{2}$$

where WTC is the wind turbine capacity, r is the Banki turbine's radius, and η is the efficiency. The needed solar PV panels power is calculated via the equation [12]:

$$PVW = \frac{DL}{SDH \times LF \times PR} \tag{3}$$

where PVW is the solar PV power, DL is the daily load, SDH is the sun daily hours, LF is the losses factor, and PR is the performance ratio. The PV module power capacity is computed using the formula:

$$P_{PV} = \frac{P_{Load}}{\eta_{Module} \times \eta_{Charge\ Controller} \times \eta_{Battery} \times \eta_{Cables}} \tag{4}$$

The overall watt peak needed for the PV module, P_{Peak} is computed using the formula:

$$P_{Peak} = \frac{P_{PV}}{SDH} \tag{5}$$

To calculate the battery amperage, the following equation is used [13]:

$$BAC = \frac{DHL \times AD}{B_{Loss} \times DOD \times NV} \tag{6}$$

where BAC is the battery amperage capacity, DHL is the daily hourly load, AD is the autonomy days, DOD is the depth of discharge, B_{Loss} is the battery loss factor, and NV is the battery's nominal voltage. The charge controller current, CCC, is calculated using the equation:

$$CCC = (NS)(SCC)(LF) \tag{7}$$

where NS is the number of strings, SCC is the short circuit current, and LF is the average losses.

4. Experimental procedure and setup

4.1. Systems components design

4.1.1. Wind turbine design

Based on the measured wind data at the site, the Banki-Darius wind turbine was designed. The Banki wind turbine comprised of two layers, one on top of the other. Each layer had 8 blades. The diameter of the Banki wind turbine is 39 cm, with a total height of 68.5 cm. This yielded a wing area of 0.2672 m². The response speed of the Banki wind turbines is between 5 and 25 m/s [14]. Noting that the density of air is 1.22 kg/m^3 at an atmospheric pressure of 101.325 kPa [15], the maximum efficiency of the combined wind turbine is estimated to be 56.64%, according to the Betz limit [16]. Substituting all values of these parameters into Eq 1 resulted in a wind power of 12.22 W and 1,528.10 W for wind speeds of 5 and 25 m/s, respectively. However, the maximum wind speed recorded in the year 2021 at the site was 12.10 m/s, which provided a maximum power of the wind turbine of about 113 W. Figure 1 shows the fabrication and design processes for the combined Banki-Darrieus wind turbine.

Figure 1. The manufacturing and designing processes of the combined Banki-Darrieus wind turbine.

To generate more efficient electrical power from wind power, three Darieus wind blades positioned between the hub height were incorporated into the Banki wind turbine to form the combined wind system, as shown in Figure 2. The capacity of the combined wind turbine can reach 300 Watt.

Figure 2. The overall system's components.

Table 1 presents the combined Banki-Darrieus wind turbine data.

Table 1. Combined Banki-Darrieus wind turbine datasheet.

Technical specifications	Numerical value
Rotor diameter	390 mm
Hub height	685 mm
Expected lifetime	20 years
Replacement cost	100 USD
Expected O&M cost	5.0 USD/annum

4.1.2. PV system

According to the solar irradiation data measured at the experimental site, the required solar PV power (PVW), daily load, DL, sun daily hours, SDH, losses factor, LF, and performance ratio, PR, are estimated. DL is 300 Watt. Hour/day (30 Watt multiplied by 10 hours), SDH is 5.7 hours/day [16]. LF is 0.8, and PR is 0.85. Substituting these value leads to a PVW of 77.4 Watt.

Table 2. 80-Watt PV module specifications.

Technical specifications	Numerical value
Maximum power	80 Watt
Number of PV panels	2
Tolerance	$\pm$ 3 percent
Open circuit voltage	22 Volts
Short circuit current	4.85 Ampere
Maximum power voltage	18 Volts
Maximum power current	4.44 Ampere
PV panel efficiency	13.05 Percent
Solar cell efficiency	17.2 Percent
Series fuse rating	15 Ampere
Junction box protection	IP65
Maximum system voltage	1,000 Volt DC
Operating temperature	−40 ℃ to 85 ℃
Dimensions	915 mm × 670 mm × 30 mm
Weight	7.31 kg

To calculate the P_{PV}, Eq 4 parameters are substituted, P_{Load} = 300 Wh/day, η_{Module} as 0.85, $\eta_{Charge\ Controller}$ as 0.95, $\eta_{Battery}$ as 0.85, and η_{Cables} as 0.97 into the previous equation leads to 450.6 Wh/day. Thus, the total power rating of the PV panels, P_{Peak}, equals 79.1 Watts.

To generate clean electricity from solar radiation, an 80 Watts solar PV polycrystalline CENTSYS module was therefore selected. However, a second 80W PV module was added in order to enhance charging of the battery for longer runtime at times of low solar irradiation.

The datasheet of the 80-Watt PV module is represented in Table 2.

4.1.3. Battery

To select the battery, Eq 6 was used to determine the amperage of the battery. Substituting the values of Eq 6 is based on DHL of 300 Wh, AD is 3 days, B_{Loss} is 0.85 according to the high temperature losses at the site weather conditions, DOD was assumed 60%, and NV of 12 V leads to BAC of 147 Ah. Thus, 150 Ah Gel battery was chosen, the specifications and datasheet of the Gel battery used in the hybrid energy system are presented in Table 3.

Table 3. 80-Watt PV panel specifications.

Technical specifications	Characterization
Model number	SB150
Storage system category	Standalone (Off-grid)
Battery type	Lithium Ion
Maximum amperage capacity	150 Ah
Nominal voltage	12 Volts
Maximum discharge current	1,500 Ampere
Battery dimensions	490.20 mm × 228.60 mm × 266.7 mm
Battery weight	295 kilograms

4.1.4. Charge controller

In this study, three charge controllers were used, one for each of the two solar PV modules and the third for the combined wind turbine. For solar PV module, the following equations present the calculations of voltage and current of the PV charge controller, which included the maximum power of PV module that is 80 Watt, the maximum voltage of PV module that is 18 Watt, and the maximum current for the PV module that is 4.44 Ampere. The open circuit voltage of the PV module is 22 Volts, and the short current circuit for the PV module is 4.85 Ampere. Substituting the previous values in Eq 7, yields:

$$CCC = (1)\ (4.85)\ (1.3) = 6.3 \text{ Ampere}$$

Therefore, the charge controller should be rated at 6.5 Ampere at the 12 Volts.

For the wind turbine, based on data on a 300 W catalogue of vertical axis wind turbine, the charge controller voltage is 12 volts, whilst the open circuit current is less than 20 Ampere.

A charge controller is used in this system to provide protection for the lithium-ion battery used to store electrical energy. Charge controller can prevent battery from high level of depth of discharge (DOD), and high level of state of charge (SOC), which can help maintain high lifespan of the battery [17]. The charge controllers used in this study for both solar PV modules and the combined Banki-Darrieus wind turbine are shown in Figure 3.
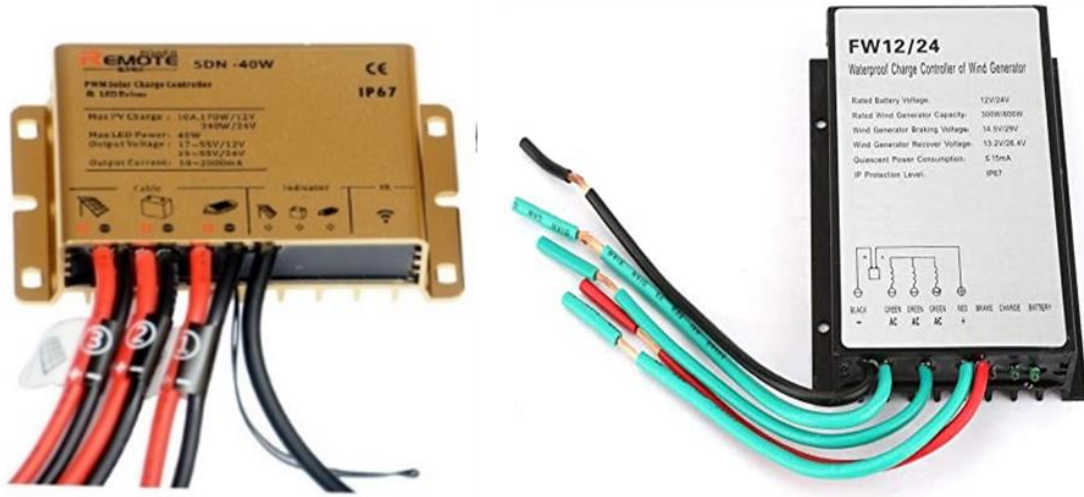
Figure 3. Charge controller used in this study for (PV panel on the left) and (wind turbine on the right).

4.2. The overall system configuration

The overall system's components are presented in Figure 3 above. Whereas, the electrical connection of the hybrid solar-wind system is shown in Figure 4, in which the PV module one and the combined wind turbine system work for providing extra electrical charge for the battery, while the PV module two is the one in charge of lighting the LED light at night by the battery and through its charge controller.
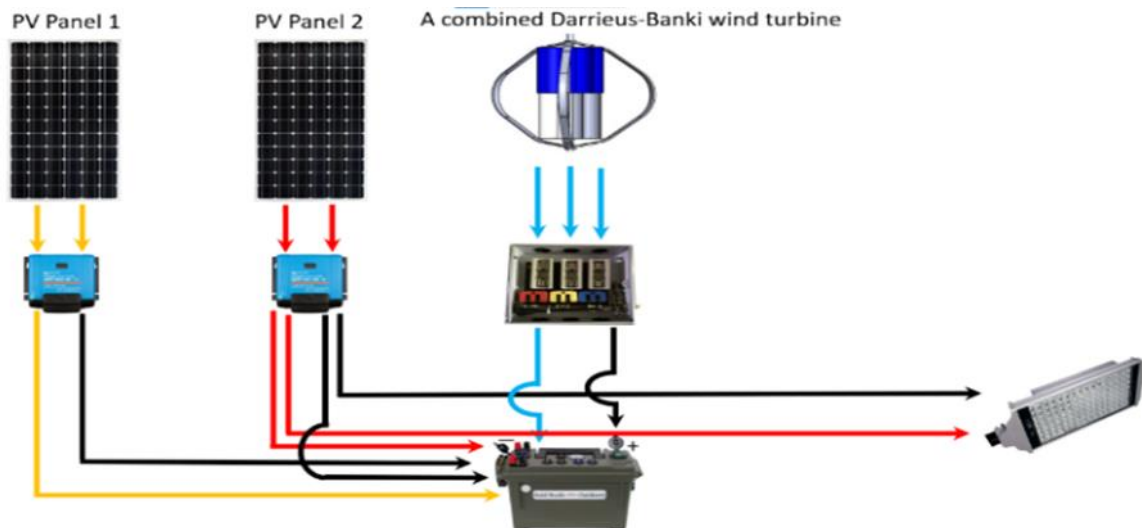
Figure 4. Configuration of PV-wind street lighting system.

5. Results and discussions

This section presents the experimental and numerical results obtained in this work.

5.1. Experimental results

Figure 5 indicates that the average power that could be obtained from the wind speed, which ranges between 30 and 120 Watt.
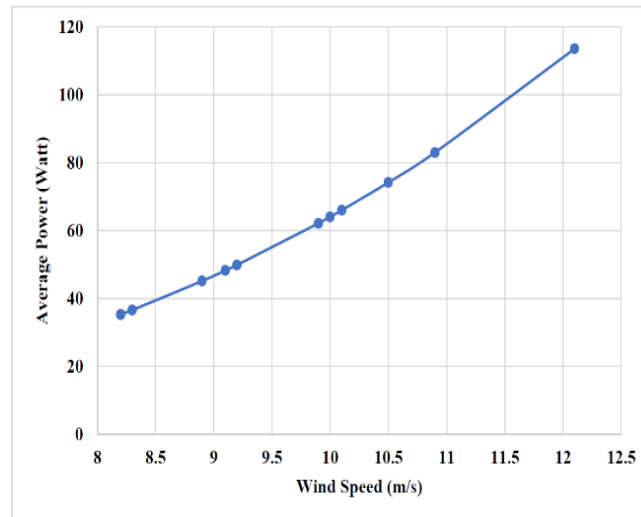
Figure 5. Average power obtained from the wind speed at Mutah University site.
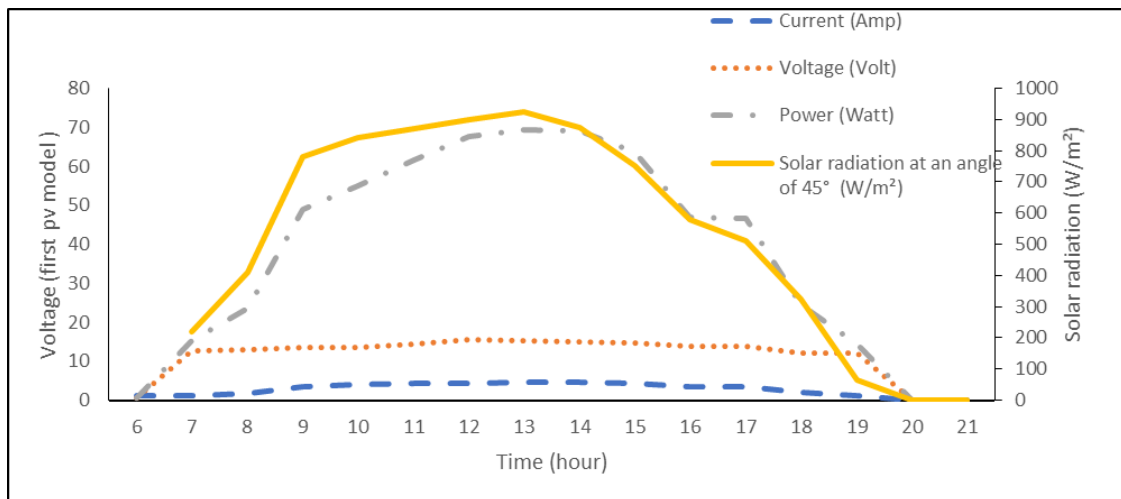
Figure 6. Solar irradiation, current, voltage, and power of the first PV module measured on August 26, 2021.

The maximum value of average power in the year 2021 was recorded at a wind speed of approximately 12 m/s, whilst the minimum average power of wind was recorded at a wind speed of approximately 8 m/s.

Figure 6 presents the solar irradiation, current, voltage, and power of the first PV module used in the experimental system.

It is indicated from the Figure 6 that the current ranged between around 0.9 (minimum value) and 4.6 Amp (maximum value), while the voltage values ranged between around 0.7 Volts and 15.34 Volts. Correspondingly, the power values ranged between a minimum value of approximately 0.6 Watt and a maximum of 70 Watt.

Figure 7 indicates that the current of the battery load was approximately constant over the day ranging between 2.2 and 2.4 Ampere. The value of voltage varied between roughly 12.2 and 12.8 Volts, providing a power that ranged between 27 and 30 Watts.
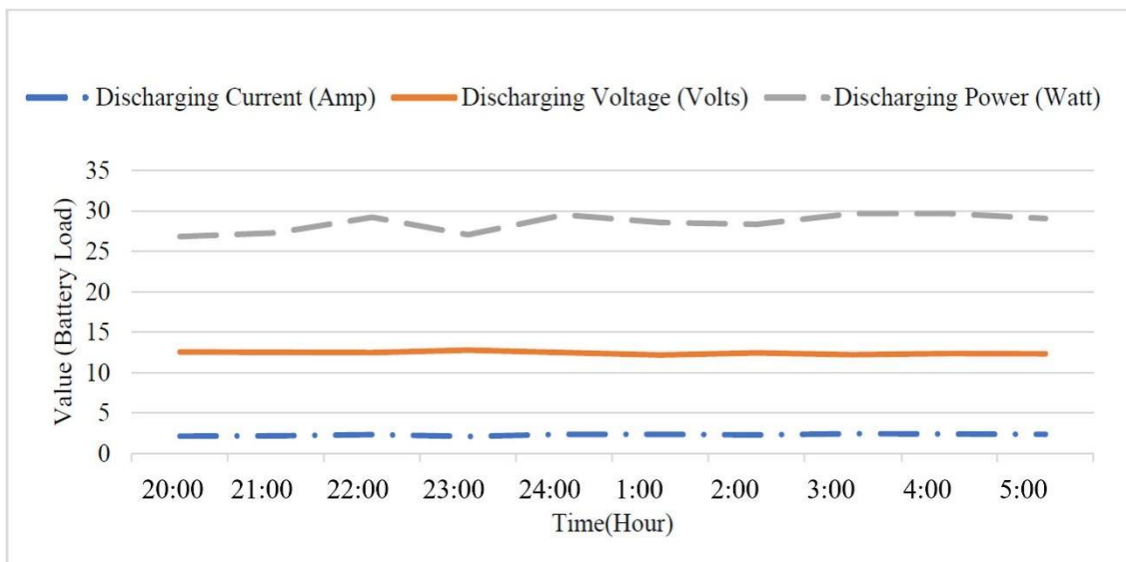
Figure 7. Battery load: current, voltage and power on August 26, 2021.
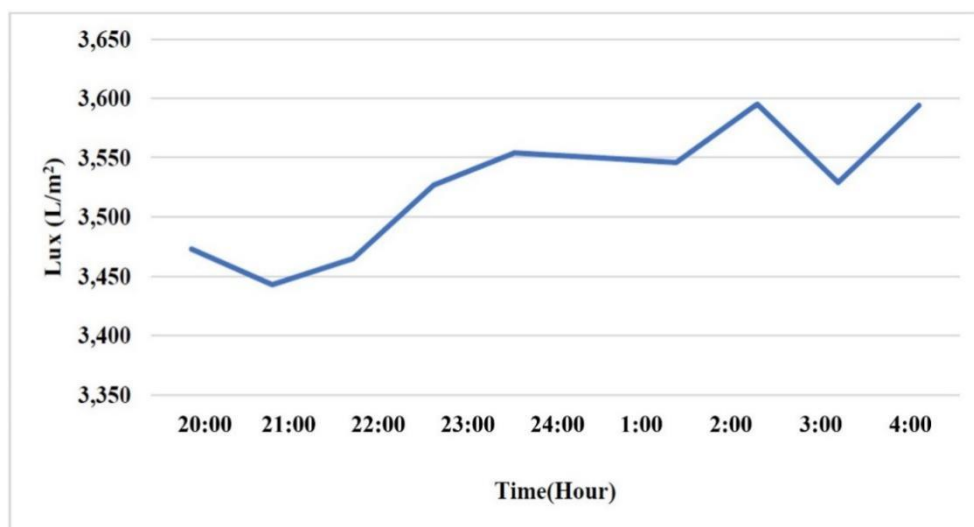
Figure 8. Light intensity at the street of the 30W LED street lamp placed at a height of 9 meters.

Figure 8 displays the light intensity at the street of the 30 W LED streetlight placed at a height of 9

meters. The figure indicates that the light intensity ranges between around 3,450 and 3,600 L/m^2, which occurs between 8:00 pm and 5:00 am. Outside this range of time, the LED streetlight provides no light intensity as it is programmed not to operate.

These results have indicated that the combined Banki-Darrieus wind turbine that included three Darrieus wind blades and two layers of the Banki wind turbine, each with eight blades, and the two PV modules, each of 80 W capacity, were appropriate to light a street LED lamp of 30 Watts.

5.2. Numerical results

After conducting optimization, sensitivity analysis, and simulation through the HOMER software package for the system presented in Figure 9, it was found that there were 3 possible scenarios of the hybrid solar PV-wind system in terms of economic feasibility. The three cases are presented in Table 4.
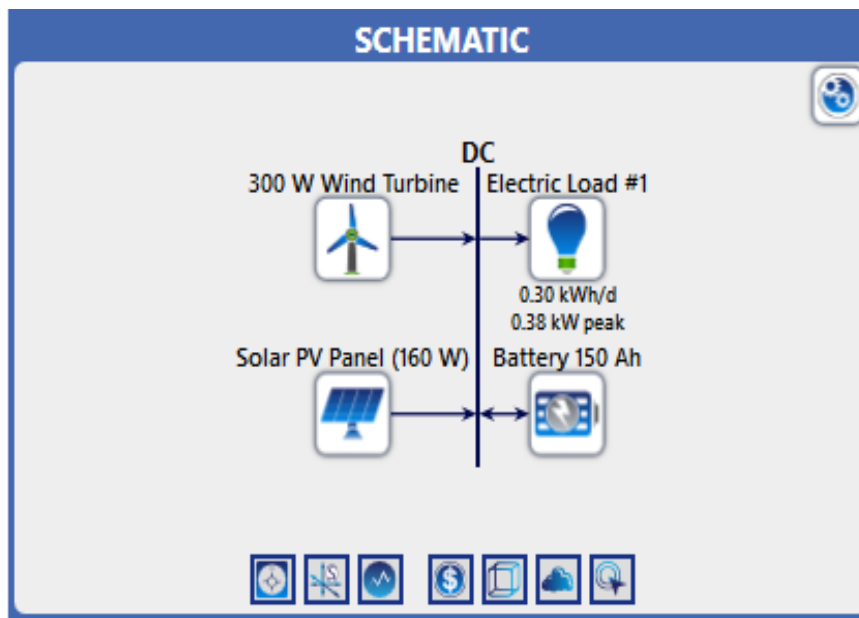
Figure 9. A schematic diagram of the hybrid solar-wind system investigated in the HOMER software.

Table 4. Scenarios defined in HOMER software.

#	Power production source	Energy storage (battery)	Layout	LCOE (USD/kWh)
1	PV Panels and Wind Turbine	Yes		0.5387
2	Only wind turbine	Yes		0.8232
3	Only PV panels	Yes		0.8791

The HOMER software numerical results revealed that the LCOE of case (1) (solar PV, wind turbine,

and battery) was 0.5387 $/kWh. The net present cost of the system equals $762.09, while the system's operating cost in this scenario equals $21.24. However, the LCOE value of scenario (2) (wind turbine and battery) was 0.8232 $/kWh, with the net present cost of the system equals $1,165.22, while the system's operating price in this scenario equals $34.05. Whereas, the LCOE was 0.8791 $/kWh for scenario (3) (PV panels and battery). The system's net present cost equals $1,243.50, while the system's operating price in this scenario equals $22.22. Surely, the software results showed that the hybrid wind-solar system is the most economically feasible case.

6. Conclusions

This experimental and numerical study investigated the suitability of a wind-solar hybrid system in lighting street LED lights on highway poles. The hybrid system includes a combined Banki-Darrieus wind turbine integrated with a PV solar system to provide energy to light a 30 W street lamp. The numerical part of this study included the use of HOMER software to check the levelized cost of energy of the hybrid system, which provided an assessment of the system's economic feasibility.

The main results of this experimental and theoretical study revealed the following findings:

1. The experimental results revealed that the design of the Banki-Darrieus wind turbine that included three Darrieus wind blades and two layers of the Banki wind turbine, each with eight blades and of a diameter of 39 cm and a total height of 68.5 cm, and the two PV modules, each of 80 W capacity, were adequate to light the 30 W LED street lamp.
2. The maximum wind speed recorded in 2021 at the experimental site was 12.10 m/s, which provided the wind turbine power of 113 Watts.
3. The HOMER software numerical results revealed that the hybrid wind-solar system is the most economically feasible case among using either wind or solar system alone.

Acknowledgements

Conflict of interest

The authors declare no conflict of interest.

Author contributions

Conception and design of study: Nadwan Majeed Ali, Handri Ammari.
Drafting the manuscript: Nadwan Majeed Ali.
Analysis and/or interpretation of data: Handri Ammari.

References

1. Khare V, Nema S, Baredar P (2016) Solar-wind hybrid renewable energy system: A review. *Renew Sustain Energy Rev* 58: 23–33. https://doi.org/10.1016/j.rser.2015.12.223

2. Al-Tarawneh L, Alqatawneh A, Tahat A, et al. (2021) Evolution of optical networks: From legacy networks to next-generation networks. *J Opt Commun* 2020. https://doi.org/10.1515/joc-2020-0108

3. Mazzeo D, Herdem MS, Matera N, et al. (2021) Artificial intelligence application for the performance prediction of a clean energy community. *Energy* 232. https://doi.org/10.1016/j.energy.2021.120999

4. Elmorshedy MF, Elkadeem MR, Kotb KM, et al. (2021) Optimal design and energy management of an isolated fully renewable energy system integrating batteries and supercapacitors. *Energy Convers Manage* 245. https://doi.org/10.1016/j.enconman.2021.114584

5. Mazzeo D, Matera N, de Luca P, et al. (2021) A literature review and statistical analysis of photovoltaic-wind hybrid renewable system research by considering the most relevant 550 articles: An upgradable matrix literature database. *J Clean Prod* 295. https://doi.org/10.1016/j.jclepro.2021.126070

6. Wadi M, Shobole A, Tur MR, et al. (2018) Smart hybrid wind-solar street lighting system fuzzy based approach: Case study Istanbul-Turkey. In: *Proceedings—2018 6th International Istanbul Smart Grids and Cities Congress and Fair, ICSG 2018*. https://doi.org/10.1109/SGCF.2018.8408945

7. Ricci R, Vitali D, Montelpare S (2015) An innovative wind-solar hybrid street light: Development and early testing of a prototype. *Int J Low-Carbon Technol* 10: 420–429. https://doi.org/10.1093/ijlct/ctu016

8. Georges S, Slaoui FH (2011) Case study of hybrid wind-solar power systems for street lighting. Published in: *2011 21st International Conference on Systems Engineering*. https://doi.org/10.1109/ICSEng.2011.22

9. AL-SARRAJ A, Salloom HT, Mohammad KK, et al. (2020) Simulation design of hybrid system (Grid/PV/Wind Turbine/battery/diesel) with applying HOMER: A case study in Baghdad, Iraq. *Int J Electron Commun Eng* 7: 10–18. https://doi.org/10.14445/23488549/IJECE-V7I5P103

10. Badger J, Frank H, Hahmann AN, et al. (2014) Wind-climate estimation based on mesoscale and microscale modeling: Statistical-dynamical downscaling for wind energy applications. *J Appl Meteorol Climatol* 53: 1901–1919. https://doi.org/10.1175/JAMC-D-13-0147.1

11. Arramach J, Boutammachte N, Bouatem A, et al. (2020) A novel technique for the calculation of post-stall aerodynamic coefficients for S809 airfoil. *FME Trans* 48: 117–126. https://doi.org/10.5937/fmet2001117A

12. Morozov VA, Yahin AM, Zhirova AE, et al. (2020) Hardware-software system for studying the effectiveness of propeller-engine groups for unmanned aerial vehicles. *J Phys: Conf Ser* 1582: 012063. https://doi.org/10.1088/1742-6596/1582/1/012063

13. Sohoni V, Gupta SC, Nema RK (2016) A critical review on wind turbine power curve modelling techniques and their applications in wind based energy systems. *J Energy*, 18. https://doi.org/10.1155/2016/8519785

14. Ranjbar MH, Zanganeh H, Gharali K, et al. (2019) Reaching the BETZ Limit experimentally and numerically. *Energy Equip Sys* 7: 271–278. https://doi.org/10.22059/ees.2019.36563

15. Alrwashdeh SS, Alsaraireh FM, Saraireh MA (2018) Solar radiation map of Jordan governorates. *Int J Eng Technol*, 7. https://doi.org/10.14419/ijet.v7i3.15557

16. Ingole JN, Choudhary MA, Kanphade RD (2012) PIC based solar charging controller for battery. *Int J Eng Sci Technol* 4: 384–390. Available from: http://www.ijest.info/abstract.php?file=12-04-02-192.